Supplemental Material: Sign-changing photon-mediated atom interactions in multimode cavity QED

Yudan Guo,[1,2] Ronen M. Kroeze,[1,2] Varun D. Vaidya,[1,2,3] Jonathan Keeling,[4] and Benjamin L. Lev[1,2,3]

[1]*Department of Physics, Stanford University, Stanford, CA 94305*
[2]*E. L. Ginzton Laboratory, Stanford University, Stanford, CA 94305*
[3]*Department of Applied Physics, Stanford University, Stanford, CA 94305*
[4]*SUPA, School of Physics and Astronomy, University of St Andrews, St Andrews KY16 9SS UK*

(Dated: February 21, 2019)

Spectrum of a confocal cavity

Within paraxial optics, the beam inside a Fabry-Pérot cavity is described by Hermite-Gaussian modes. A mode $\Phi_{Q,l,m}$ is labeled by one longitudinal index Q and two transverse indices l and m. These indices count the number of field nodes along their respective axes. For a symmetric two-mirror cavity of length L, with R as the mirror radius of curvature, the frequency of a given mode is

$$f_{Qlm} = \frac{c}{2L}\left[Q + \frac{l+m+1}{\pi}\arccos g\right], \tag{1}$$

where c is the speed of light inside the cavity, $g = 1 - L/R$ and $c/2L$ is the free spectral range of the cavity. The term proportional to $\arccos g$ captures the effect of additional Gouy phase shifts on higher-order transverse modes, which involve terms proportional to $(l + m + 1)\psi(z)$, where $\psi(z) = \arctan(z/z_R)$ is the Gouy phase and z_R is the Rayleigh range $z_R = \pi w_0^2/\lambda$.

In general, different transverse modes will be resonant at different frequencies; however, degenerate cavities with special geometries can support a family of transverse modes, each with distinct spatial profiles, at a single frequency. In particular, a confocal cavity has $L = R$ and thus $g = 0$. Therefore, all modes that satisfy the condition

$$Q + \frac{1}{2}(l + m + 1) = Q_0 + \frac{(\eta + 1)}{2} \tag{2}$$

will be resonant at the same frequency $c(2Q_0+\eta+1)/4L$, where Q_0 is a positive integer and $\eta = 0(1)$ for even (odd) families. At every half free spectral range, the transverse mode content varies between all even modes $l + m \bmod 2 = 0$ and all odd modes $l + m \bmod 2 = 1$. Within a degenerate resonance, to satisfy Eq. (2), different transverse modes must carry different longitudinal indices. This causes the longitudinal profile of sequential transverse modes within a degenerate resonance to cycle between $+\cos k_r z$, $-\sin k_r z$, $-\cos k_r z$, and $+\sin k_r z$, as described in Fig. 1(a) of the main text.

Experimental apparatus

This work employs a $R = 1$-cm radius-of-curvature confocal cavity of length $L = R$. The length of the multimode cavity is adjustable [1], though in this work we set $L = R$. The transmission spectrum of the employed near-confocal cavity is shown in Fig. 1.

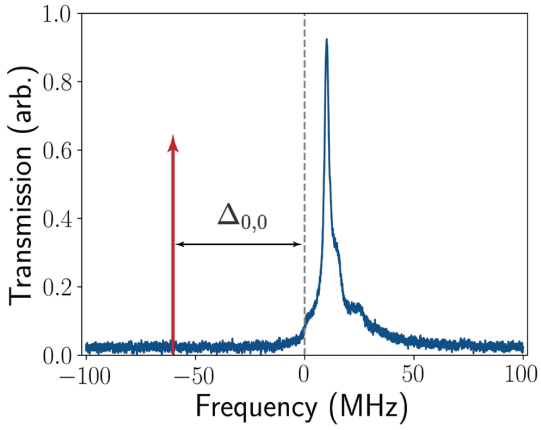

FIG. 1. Transmission spectrum of the employed near-confocal cavity. All data in the main text are taken with detuning $\Delta_{0,0} = 60$ MHz, defined from the position of the $\mathrm{TEM}_{0,0}$ resonance.

We trap within this cavity a BEC of $2.5(3)\times10^5$ Rb^{87} atoms in the $|F = 1, m_F = -1\rangle$ state. See Ref. [1] for BEC preparation procedure and Fig. 1 for illustration of experiment. The BEC is confined in a crossed optical dipole trap (ODT) formed by a pair of 1064-nm laser beams propagating along $\hat{x}$ and $\hat{y}$ with waists of 40 μm in the xy-plane and 80 μm along $\hat{z}$. The resulting trap frequencies of $(\omega_x, \omega_y, \omega_z) = 2\pi \times [189(2), 134(1), 90(1)]$ Hz create a compact BEC with Thomas-Fermi radii $(R_x, R_y, R_z) = [4.2(1), 5.8(3), 8.9(1)]$ μm that are significantly smaller than the $w_0 = 35$ μm waist of the $\mathrm{TEM}_{0,0}$ cavity mode. Note that the mode waist w_0 is defined as the e^{-2} intensity; Ref. [5] uses e^{-1} intensity, which removes the factor of 2 from the cosine argument in U_{nonlocal}.

Acousto-optic deflectors (AODs) placed in the path of each ODT control the intensity and location of the ODTs, allowing us to translate the BEC to any point in the xy-plane with an uncertainty of 0.9 μm. In the experiments of Figs. 3 and 4, we use dynamic trap shaping [2] to produce two smaller BECs of $2.0(3)\times10^5$ atoms each, with a population imbalance uncertainty of <10%. The relative

position of these BECs along $\hat{x}$ is controlled by the AOD.

Both the local oscillator beam (used for holographic imaging of the cavity emission) and the transverse pump are derived from the same laser but pass through different acousto-optic modulators (AOMs) for intensity stabilization. To maintain the relative phase stability between the two beams, both AOMs are driven by signals from the same multichannel direct digital synthesizer. This synthesizer is synced to a stable Rb frequency reference. Due to path length drift, the relative phase between the pump and the local oscillator is stable only within the same experiment realization.

Holographic imaging

The employed holographic imaging method is described in detail in Ref. [3] and is similar to that reported in Ref. [4]. Briefly, a portion of the pump field—serving as a local oscillator (LO)—is directed onto the same EMCCD camera onto which the cavity emission is imaged. The cavity field $E_c(\mathbf{r}) = |E_c(\mathbf{r})|e^{i\phi_c(\mathbf{r})}$ and the LO field $E_{\rm LO}(\mathbf{r}) = |E_{\rm LO}(\mathbf{r})|e^{i\phi_{\rm LO}(\mathbf{r})}$ interfere to form a spatial heterodyne image $I_h(\mathbf{r})$. The image's interference fringes are proportional to the phase and amplitude of the cavity field:

$$I_h(\mathbf{r}) \propto |E_c(\mathbf{r})E_{\rm LO}(\mathbf{r})| \cos\left[\Delta\mathbf{k}\cdot\mathbf{r} + \Delta\phi(\mathbf{r})\right], \qquad (3)$$

where the phase difference betwween the cavity and LO wavefronts is $\Delta\phi(\mathbf{r}) = \phi_c(\mathbf{r}) - \phi_{\rm LO}(\mathbf{r})$. The amplitude and phase of the fringes produced are a measure of $|E_c(\mathbf{r})|$ and $\phi_c(\mathbf{r})$.

Demodulating this image at the fringe wavevector $\mathbf{\Delta k}$ provides a holographic reconstruction of $|E_c(\mathbf{r})|$ and $\phi_c(\mathbf{r})$. Accurate extraction of these images requires the correction of LO intensity and phase variation. To do so for the confocal cavity, we perform a least-squares fit to the cavity emission intensity pattern using the exact theory result from Ref. [5]. We extract the LO phase variation from the difference between measured phase and the expected phase.

Effective Hamiltonian

The Green's function for the cavity-mediated interaction in a perfect confocal cavity near an even degenerate resonance can be written as a sum of the contributions from the two classes of longitudinal modes [5, 6]:

$$4\mathcal{D}^+(\mathbf{x},\mathbf{x}') = 4\mathcal{D}^+(\mathbf{r},\mathbf{r}',z,z') = D_c(\mathbf{r},\mathbf{r}')\cos k_r z\cos k_r z' + D_s(\mathbf{r},\mathbf{r}')\sin k_r z\sin k_r z', \qquad (4)$$

with

$$\begin{cases} D_c = \delta\left(\frac{\sqrt{2}(\mathbf{r}-\mathbf{r}')}{w_0}\right) + \delta\left(\frac{\sqrt{2}(\mathbf{r}+\mathbf{r}')}{w_0}\right) + \frac{1}{\pi}\cos\left(\frac{2\mathbf{r}\cdot\mathbf{r}'}{w_0^2}\right) \\ D_s = \delta\left(\frac{\sqrt{2}(\mathbf{r}-\mathbf{r}')}{w_0}\right) + \delta\left(\frac{\sqrt{2}(\mathbf{r}+\mathbf{r}')}{w_0}\right) - \frac{1}{\pi}\cos\left(\frac{2\mathbf{r}\cdot\mathbf{r}'}{w_0^2}\right). \end{cases} \qquad (5)$$

To allow for the full phase freedom in the atomic density wave, the atomic profile is expanded as

$$\Psi(\mathbf{x}) = \sqrt{\rho(\mathbf{r}-\mathbf{r}_0)}\times \left[\psi_0 + \sqrt{2}\cos k_r x(\psi_c\cos k_r z + \psi_s \sin k_r z)\right], \qquad (6)$$

where $\mathbf{r}_0$ is the location of the atoms in the cavity transverse plane, ψ_0 is the ground state fraction of the gas that has a uniform density profile (compared to the λ-scale) and $\psi_{c(s)}$ is the excited atomic density wave in the $\cos k_r z$ ($\sin k_r z$) pattern. The Hamiltonian is then

$$H = E_0\int d^3\mathbf{x}d^3\mathbf{x}'\cos(k_r x)\cos(k_r x')\times |\Psi(\mathbf{x})|^2\mathcal{D}^+(\mathbf{x},\mathbf{x}')|\Psi(\mathbf{x}')|^2 \equiv -E_0\mathcal{H}, \qquad (7)$$

where E_0 is a positive constant prefactor that absorbs parameters such as pump strength and cavity single photon Rabi rate g_0, and $\cos(k_r x)\cos(k_r x')$ term is due to the standing wave pump. To proceed, we note the length scale separation $\lambda \ll r_{\rm TF} \ll w_0$, where $r_{\rm TF}$ is the Thomas-Fermi radius of the condensate. This allows us to drop the fast oscillating terms due to the pump and cavity longitudinal profile. The second inequality means that we can treat the density profile $\rho(\mathbf{r})$ as a δ-function when evaluating terms that varies on the scale of the cavity waist w_0. Since D_c and D_s have identical contribution from local interactions (δ-function part) and we are interested in the choice between ψ_c and ψ_s density waves, focusing only on the nonlocal interaction terms involving $\cos(2\mathbf{r}\cdot\mathbf{r}'/w_0^2)$ in $\mathcal{D}^+(\mathbf{x},\mathbf{x}')$, the effective Hamiltonian $\mathcal{H}$ can be evaluated as

$$\mathcal{H} = -\frac{1}{2\pi}\left[|\psi_0\psi_c|^2 - |\psi_0\psi_s|^2\right]\cos\left(\frac{2r_0^2}{w_0}\right), \qquad (8)$$

where we have taken ψ_0 and $\psi_{c,s}$ to be real in the small dissipation limit. Defining the following order parameters

$$\chi_c = \frac{\psi_0\psi_c}{N}, \qquad \chi_s = \frac{\psi_0\psi_s}{N}, \qquad (9)$$

and ignoring the numeric prefactor, we recover the effective Hamiltonian in the main text, where N is the total atom number. For two BECs, the cross term in the integral in Eq. 7 gives rise to the interaction term

$$H_{12} \propto -J_{12}(\chi_{c1}\chi_{c2} - \chi_{s1}\chi_{s2}), \qquad (10)$$

where $J_{12} = 2N\cos\left(2\mathbf{r_1}\cdot\mathbf{r_2}/w_0^2\right)$.

[1] A. J. Kollár, A. T. Papageorge, K. Baumann, M. A. Armen, and B. L. Lev, "An adjustable-length cavity and

Bose-Einstein condensate apparatus for multimode cavity QED," New J. Phys. **17**, 43012 (2015).

[2] K. Henderson, C. Ryu, C. MacCormick, and M. G. Boshier, "Experimental demonstration of painting arbitrary and dynamic potentials for Bose-Einstein condensates," New J. Phys. **11**, 043030 (2009).

[3] R. M. Kroeze, Y. Guo, V. D. Vaidya, J. Keeling, and B. L. Lev, "Spinor Self-Ordering of a Quantum Gas in a Cavity," Phys. Rev. Lett. **121**, 163601 (2018).

[4] N. Schine, M. Chalupnik, T. Can, A. Gromov, and J. Simon, "Electromagnetic and gravitational responses of photonic Landau levels," Nature **565**, 173 (2019).

[5] V. D. Vaidya, Y. Guo, R. M. Kroeze, K. E. Ballantine, A. J. Kollár, J. Keeling, and B. L. Lev, "Tunable-Range, Photon-Mediated Atomic Interactions in Multimode Cavity QED," Phys. Rev. X **8**, 011002 (2018).

[6] Y. Guo, V. D. Vaidya, R. M. Kroeze, R. A. Lunney, B. L. Lev, and J. Keeling, "Emergent and broken symmetries of atomic self-organization arising from Gouy phases in multimode cavity QED," (2018), arXiv:1810.xxxx.